Chapter 4.

SOLAR CELL OPERATIONAL PRINCIPLES

4.1 Basic operational principles

The working principle of all today solar cells is essentially the same. It is based on the ***photovoltaic effect***. In general, the photovoltaic effect means the generation of a potential difference at the junction of two different materials in response to visible or other radiation. The basic processes behind the photovoltaic effect are:

1. generation of the charge carriers due to the absorption of photons in the materials that form a junction,
2. subsequent separation of the photo-generated charge carriers in the junction,
3. collection of the photo-generated charge carriers at the terminals of the junction.

In general, a solar cell structure consists of an absorber layer, in which the photons of an incident radiation are efficiently absorbed resulting in a creation of electron-hole pairs. In order to separate the photo-generated electrons and holes from each other, the so-called "semi-permeable membranes" are attached to the both sides of the absorber[1]. The important requirement for the semi-permeable membranes is that they selectively allow only one type of charge carrier to pass through. An important issue for designing an efficient solar cell is that the electrons and holes generated in the absorber layer reach the membranes. This requires that the diffusion lengths of the charge carriers are larger than the thickness of the absorber.

[1] P. Würfel, Physics of Solar Cells: From Principles to New Concepts, Wiley-WCH, Weinheim, 2005.

A membrane that let electrons go through and blocks holes is a material, which has a large conductivity for electrons and a small conductivity of holes. An example of such a material is an *n*-type semiconductor, in which a large electron conductivity with respect to the hole conductivity is caused namely by a large difference in electron and hole concentrations. Electrons can easily flow through the *n*-type semiconductor while the transport of holes, which are the minority carriers in such material, is due to the recombination processes very limited. The opposite holds for electrons in a *p*-type semiconductor, which is an example of the hole membrane.

In order to minimize the injection of holes from the absorber into the *n*-type semiconductor an energy barrier should be introduced in the valence band, E_V, between the *n*-type semiconductor and the absorber. Ideally, this can be achieved by choosing an *n*-type semiconductor that has a larger band gap than that of the absorber and the energy difference is located in the valence band of the two materials. Similarly, the injection of electrons from the absorber into the *p*-type semiconductor could be suppressed by using a *p*-type semiconductor with a larger band gap than that of the absorber and having the band off-set in the conduction band, E_C, between the absorber and the *p*-type semiconductor. The requirement of having the band off-set in the conduction band means that the electron affinity, χ_e, of the *p*-type semiconductor is smaller that the electron affinity of the absorber. The additional advantage applying membrane materials with large band gaps is to allow almost all photons to be transmitted and absorbed into the absorber.

The asymmetry in the electronic structure of the *n*-type and *p*-type semiconductors is the basic requirement for the photovoltaic energy conversion. Figure 4.1 shows a schematic band diagram of an illuminated idealized solar cell structure with an absorber and the semi-permeable membranes at two conditions. The quasi-Fermi level for electrons, E_{FC}, and the quasi-Fermi level for holes, E_{FV}, are used to describe the illuminated state of the solar cell. The energy difference between the quasi-Fermi levels is a measure of efficient conversion of energy of radiation into electrochemical energy.

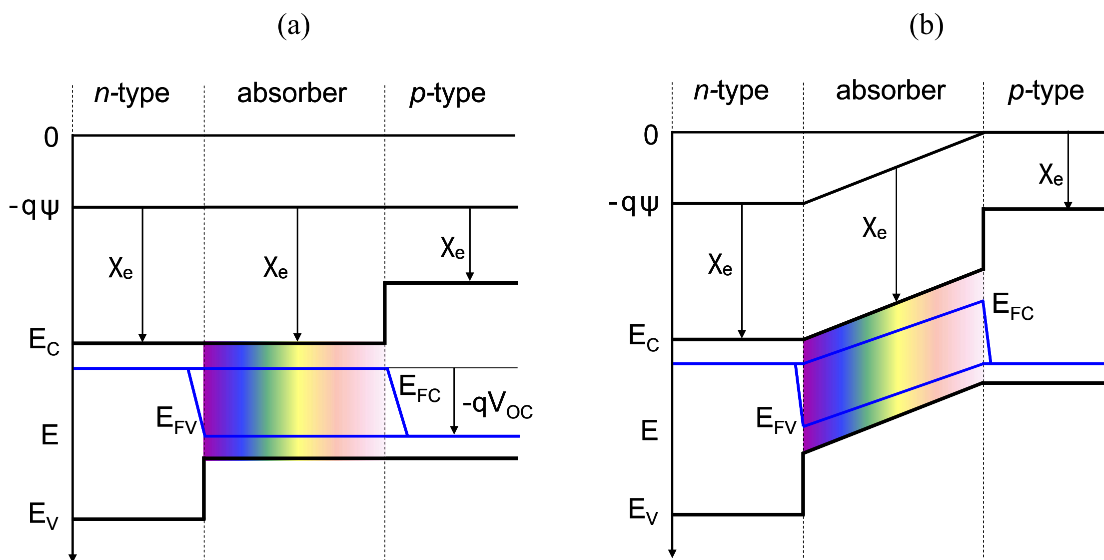

Figure 4.1. Band diagram of an idealized solar cell structure at the a) open-circuit and b) short-circuit conditions.

4.2 The *p-n* junction

At present, the most frequent example of the above-described solar cell structure is realized with crystalline silicon (c-Si). A typical c-Si solar cell structure is shown in Figure 3.1. A moderately-doped *p*-type c-Si with an acceptor concentration of 10^{16} cm^{-3} is used as an absorber. On the top side of the absorber a thin, less than 1 μm thick, highly-doped *n*-type layer is formed as the electron membrane. On the back side of the absorber a highly-doped *p*-type serves as the hole membrane. At the interfaces between the c-Si *p*-type absorber and the highly-doped *n*-type and *p*-type membranes, regions are formed with an internal electric field. These regions are especially important for solar cells and are known as ***p-n* junctions**. The presence of the internal electric field in the solar cell facilitates the separation of the photo-generated electron-hole pairs. When the charge carriers are not separated from each other in a relatively short time they will be annihilated in a process that is called recombination and thus will not contribute to the energy conversion. The easiest way to separate charge carriers is to place them in an electric field. In the electric field the carriers having opposite charge are drifted from each other in opposite directions and can reach the electrodes of the solar cell. The electrodes are the metal contacts that are attached to the membranes.

The *p-n* junction fabricated in the same semiconductor material such as c-Si is an example of the *p-n* homojunction. There are also other types of a junction that result in the formation of the internal electric field in the junction. The *p-n* junction that is formed by two chemically different semiconductors is called the *p-n* heterojunction. In the *p-i-n* junctions, the region of the internal electric field is extended by inserting an intrinsic, *i*, layer between the *p*-type and the *n*-type layers. The *i*-layer behaves like a capacitor and it stretches the electric field formed by the *p-n* junction across itself. Another type of the junction is a junction between a metal and a semiconductor, MS junction. The Schottky barrier formed at the metal-semiconductor interface is a typical example of the MS junction.

4.2.1 Formation of a space-charge region in the *p-n* junction

Figure 4.2 shows schematically isolated pieces of a *p*-type and an *n*-type semiconductor and their corresponding band diagrams. In both isolated pieces the charge neutrality is maintained. In the *n*-type semiconductor the large concentration of negatively-charged free electrons is compensated by positively-charged ionized donor atoms. In the *p*-type semiconductor holes are the majority carriers and the positive charge of holes is compensated by negatively-charged ionized acceptor atoms. For the isolated *n*-type semiconductor we can write:

$$n = n_{n0} \approx N_D \quad (4.1a)$$

$$p = p_{n0} \approx n_i^2 / N_D \,. \quad (4.1b)$$

For the isolated *p*-type semiconductor

$$p = p_{p0} \approx N_A \quad (4.2a)$$

$$n = n_{p0} \approx n_i^2 / N_A \,. \quad (4.2b)$$

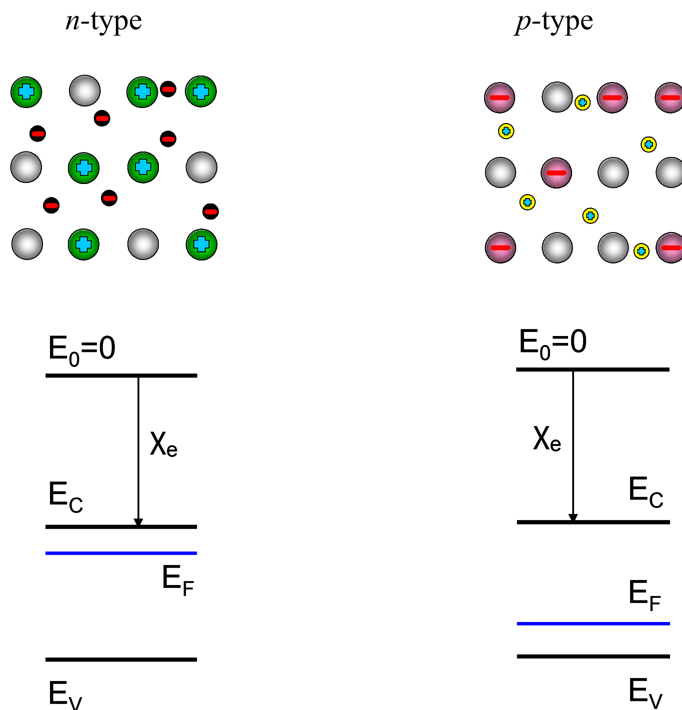

Figure 4.2. Schematic representation of an isolated *p*-type and *n*-type semiconductor and corresponding band diagrams.

When a *p*-type and an *n*-type semiconductor are brought together, a very large difference in electron concentration between *n*- and *p*-type semiconductors causes a diffusion current of electrons from the *n*-type material across the metallurgical junction into the *p*-type material. Similarly, the difference in hole concentration causes a diffusion current of holes from the *p*- to the *n*-type material. Due to this diffusion process the region close to the metallurgical junction becomes almost completely depleted of mobile charge carriers. The gradual depletion of the charge carriers gives rise to a space charge created by the charge of the ionized donor and acceptor atoms that is not compensated by the mobile charges any more. This region of the space charge is called the ***space-charge region*** or ***depleted region*** and is schematically illustrated in Figure 4.3. Regions outside the depletion region, in which the charge neutrality is conserved, are denoted as the ***quasi-neutral regions***.

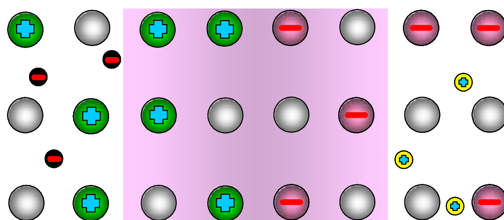

Figure 4.3. Formation of a space-charge region, when *n*-type and *p*-type semiconductors are brought together to form a junction. The colored part represents the space-charge region.

The space charge around the metallurgical junction results in the formation of an internal electric field which forces the charge carriers to move in the opposite direction than the concentration gradient. The diffusion currents continue to flow until the forces acting on the charge carriers, namely the concentration gradient and the internal electrical field, compensate each other. The driving force for the charge transport does not exist any more and no net current flows through the *p-n* junction.

4.2.2 *p-n* junction under equilibrium

The *p-n* junction represents a system of charged particles in diffusive equilibrium in which the electrochemical potential is constant and independent of position. The electrochemical potential describes an average energy of electrons and is represented by the Fermi energy. It means that under equilibrium conditions the Fermi level has constant position in the band diagram of the *p-n* junction. Figure 4.4 shows the energy-band diagram of a *p-n* junction under equilibrium. The distance between the Fermi level and the valence and/or conduction bands does not change in the quasi-neutral regions and is the same as in the isolated *n*- and *p*-type semiconductors. Inside the space-charge region, the conduction and valence bands are not represented by straight horizontal lines any more but they are curved. This indicates the presence of an electric field in this region. Due to the electric field a difference in the electrostatic potential is created between the boundaries of the space-charge region. Across the depletion region the changes in the carriers concentration are compensated by changes in the electrostatic potential. The electrostatic-potential profile is included in Figure 4.4.

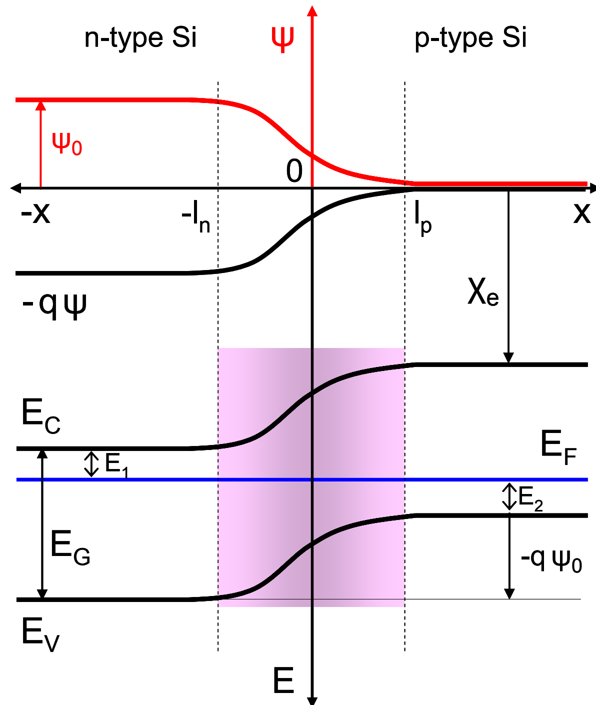

Figure 4.4. Energy-band diagram of the p-n junction. The electrostatic potential profile (red curve) is also presented in the figure.

The concentration profile of charge carriers in a *p-n* junction is schematically presented in Figure 4.5. In the quasi-neutral regions the concentration of electrons and holes is the same as in the isolated doped semiconductors. In the space-charge region the concentrations of majority charge carriers decrease very rapidly. This fact allows us to use the assumption that the space-charge region is depleted of mobile charge carriers. This assumption means that the charge of the mobile carriers represents a negligible contribution to the total space charge in the depletion region. The space charge in this region is fully determined by the ionized dopant atoms fixed in the lattice.

The presence of the internal electric field inside the *p-n* junction means that there is an electrostatic potential difference, ψ_0, across the space-charge region. We shall determine a profile of the internal electric field and electrostatic potential in the *p-n* junction. First we introduce an approximation, which simplifies the calculation of the electric field and electrostatic-potential. This approximation (*the depletion approximation*) assumes that the space-charge density, ρ, is zero in the quasi-neutral regions and it is fully determined by the concentration of ionized dopants in the depletion region. In the depletion region of the *n*-type semiconductor it is the concentration of positively charged donor atoms, N_D, which determines the space charge in this region. In the *p*-type semiconductor, the concentration of negatively charged acceptor atoms, N_A, determines the space charge in the depletion region. This is illustrated in Figure 4.6. Further, we assume that the *p-n* junction is a step junction; it means that there is an abrupt change in doping at the metallurgical junction and the doping concentration is uniform both in the *p*-type and the *n*-type semiconductors.

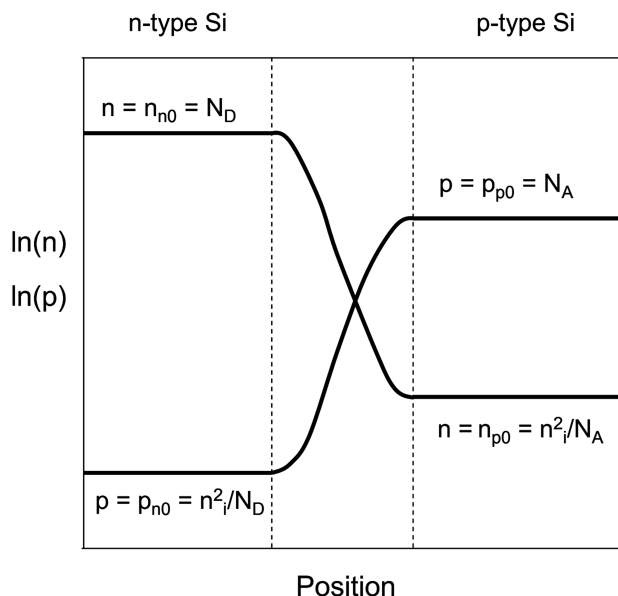

Figure 4.5. Concentrations profile of mobile charge carriers in a *p-n* junction under equilibrium.

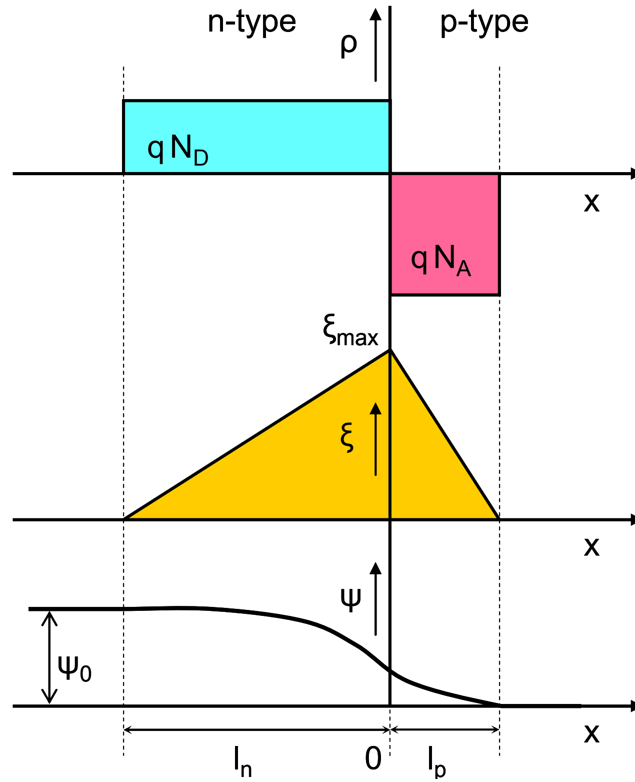

Figure 4.6. a) Space-charge density $\rho(x)$; b) electric field $\xi(x)$; c) electrostatic potential $\psi(x)$ across the depletion region of a *p-n* junction under equilibrium.

According to Figure 4.6 the position of the metallurgical junction is placed at zero, the width of the space-charge region in the *n*-type material is denoted as l_n and the width of the space-charge region in the *p*-type material is denoted as l_p. The space-charge density is described by following equations:

$$\rho(x) = q N_D \qquad \text{for } -l_n \le x \le 0 \qquad (4.3a)$$

$$\rho(x) = -q N_A \qquad \text{for } 0 \le x \le l_p \qquad (4.3b)$$

N_D and N_A is the concentration of donor and acceptor atoms, respectively. Outside the space-charge region the space-charge density is zero.

The electric field is can be calculated from the Poisson' s equation, which has the following form for one dimensional analysis:

$$\frac{d^2\psi}{dx^2} = -\frac{d\xi}{dx} = -\frac{\rho}{\varepsilon_r \varepsilon_0}. \qquad (4.4)$$

In Eq. (4.4) ψ is the electrostatic potential, ξ is the electric field, ρ is the space-charge density, ε_r is the semiconductor dielectric constant and ε_0 is the permittivity of the vacuum. For crystalline Si ε_r = 11.7 and the permittivity of the vacuum $\varepsilon_0 = 8.854\text{x}10^{-14}$ F/cm. The electric field profile can be found by integrating the space-charge density across the space-charge region.

$$\xi = \frac{1}{\varepsilon_r \varepsilon_0} \int \rho \, dx \tag{4.5}$$

Substituting the space-charge density with Eqs. (4.3a) and (4.3b) and using the following boundary conditions:

$$\xi(-l_n) = \xi(l_p) = 0 \, , \tag{4.6}$$

the solution for the electric field is

$$\xi(x) = \frac{q}{\varepsilon_r \varepsilon_0} N_D (l_n + x) \qquad \text{for } -l_n \le x \le 0 \tag{4.7a}$$

$$\xi(x) = \frac{q}{\varepsilon_r \varepsilon_0} N_A (l_p - x) \qquad \text{for } 0 \le x \le l_p \tag{4.7b}$$

At the metallurgical junction, $x = 0$, the electric field is continuous, which requires that the following condition has to be fulfilled

$$N_A l_p = N_D l_n \tag{4.8}$$

Outside the space-charge region the material is electrically neutral and therefore the electric field is zero there.

The profile of the electrostatic potential is calculated by integrating the electric field throughout the space-charge region and applying the boundary conditions.

$$\psi = -\int \xi \, dx \tag{4.9}$$

We define the zero electrostatic potential level at the outside edge of the *p*-type semiconductor. Since we assume no potential drop across the quasi-neutral region the electrostatic potential at the boundary of the space-charge region in the *p*-type material is also zero

$$\psi(l_p) = 0 \, . \tag{4.10}$$

Using Eqs. 4.6a and 4.6b for describing the electric field in the *n*-type and *p*-type parts of the space-charge region, respectively, and taking into account that at the metallurgical junction the electrostatic potential is continuous, the solution for the electrostatic potential can be written as:

$$\psi(x) = -\frac{q}{2\varepsilon_r \varepsilon_0} N_D \, (x + l_n)^2 + \frac{q}{2\varepsilon_r \varepsilon_0}\left(N_D l_n^2 + N_A l_p^2\right) \qquad \text{for } -l_n \le x \le 0 \qquad (4.11a)$$

$$\psi(x) = \frac{q}{2\varepsilon_r \varepsilon_0} N_A \left(x - l_p\right)^2 \qquad \text{for } 0 \le x \le l_p \qquad (4.11b)$$

Under equilibrium a difference in electrostatic potential, ψ_0, develops across the space-charge region. The electrostatic potential difference across the *p-n* junction is an important characteristic of the junction and is denoted as the ***built-in potential*** or ***diffusion potential*** of the *p-n* junction. We can calculate ψ_0 as the difference between the electrostatic potential at the edges of the space-charge region:

$$\psi_0 = \psi(-l_n) - \psi(-l_p) = \psi(-l_n) \qquad (4.12)$$

Using Eq. 4.11a we obtain for the built-in potential the following expression:

$$\psi_0 = \frac{q}{2\varepsilon_r \varepsilon_0}\left(N_D l_n^2 + N_A l_p^2\right). \qquad (4.13)$$

Another way to determine the built-in potential ψ_0 is to use the energy-band diagram presented in Figure 4.4.

$$q\psi_0 = E_G - E_1 - E_2 \qquad (4.14)$$

Using Eq. (3.1) and Eqs (3.18a) and (3.18b), which determine the band gap, and the positions of the Fermi energy in the *n*-type and *p*-type semiconductor, respectively,

$$E_G = E_C - E_V$$
$$E_1 = E_C - E_F = kT \ln\left(N_C / N_D\right)$$
$$E_2 = E_F - E_V = kT \ln\left(N_V / N_A\right)$$

we can write

$$q\psi_0 = E_G - kT \ln\left(\frac{N_V}{N_A}\right) - kT \ln\left(\frac{N_C}{N_D}\right) = E_G - kT \ln\left(\frac{N_V \, N_C}{N_A \, N_D}\right) \qquad (4.15)$$

Using the relationship between the intrinsic concentration, n_i and the band gap, E_G, (Eq. (3.6))

$$n_i^2 = N_C \, N_V \exp\left[-E_G / kT\right],$$

we can rewrite Eq. (4.15) to obtain

$$\psi_0 = \frac{kT}{q} \ln\left(\frac{N_A \, N_D}{n_i^2}\right). \qquad (4.16)$$

Eq. (4.16) allows us to determine the built-in potential of a *p-n* junction from the standard semiconductor parameters, such as doping concentrations and the intrinsic carrier concentration. When knowing the built-in potential we can calculate the width of the space charge region of the *p-n* junction in the thermal equilibrium. Substituting ψ_0 using Eq. (4.16) into Eq. (4.13) and taking the condition (4.7) into account, the resulting expressions for l_n and l_p are obtained. The full derivation can be found for example in reference[2].

$$l_n = \sqrt{\frac{2\varepsilon_r \varepsilon_0}{q}\psi_0 \frac{N_A}{N_D}\left(\frac{1}{N_A + N_D}\right)} \tag{4.17a}$$

$$l_p = \sqrt{\frac{2\varepsilon_r \varepsilon_0}{q}\psi_0 \frac{N_D}{N_A}\left(\frac{1}{N_A + N_D}\right)} \tag{4.17b}$$

The total space-charge width, W, is the sum of the partial space-charge widths in the *n*-type and *p*-type semiconductors and can be calculated using Eq. (4.18).

$$W = l_n + l_p = \sqrt{\frac{2\varepsilon_r \varepsilon_0}{q}\psi_0 \left(\frac{1}{N_A} + \frac{1}{N_D}\right)} \tag{4.18}$$

The space-charge region is not uniformly distributed in the *n*-type and *p*-type regions. The widths of the space-charge region in the *n*-type and *p*-type semiconductor are determined by the doping concentrations as illustrated by Eqs. (4.17a) and (4.17b), respectively. Knowing the expressions for l_n and l_p we can determine the maximum value of the internal electric field, which is at the metallurgical junction. By substituting l_p expressed by Eq (4.17b) into Eq. (4.7b) we obtain the expression for the maximum value of the internal electric field.

$$\xi_{\max} = \sqrt{\frac{2q}{\varepsilon_r \varepsilon_0}\psi_0 \left(\frac{N_A N_D}{N_A + N_D}\right)} \tag{4.19}$$

---

[2] D.A. Neaman, Semiconductor Physics and devices: Basic Principles, McGraw-Hill, 2003.

EXAMPLE

A crystalline silicon wafer is doped with 1×10^{16} acceptor atoms per cubic centimetre. A 1 micrometer thick emitter layer is formed at the surface of the wafer with a uniform concentration of 1×10^{18} donors per cubic centimetre. Assume a step p-n junction and that all doping atoms are ionized. The intrinsic carrier concentration in silicon at 300 K is 1.5×10^{10} cm^{-3}.

Let's calculate the electron and hole concentrations in the p-type and n-type quasi-neutral regions at thermal equilibrium. We shall use Eqs. (4.1a,b) and Eqs. (4.2a,b) to calculate the charge carrier concentrations.

P-type region:

$p = p_{p0} \approx N_A = 1\times 10^{16}\ cm^{-3}$.

$$n = n_{p0} = n_i^2 / p_{p0} = \left(1.5\times10^{10}\right)^2 / 10^{16} = 2.25\times10^{4}\ cm^{-3}$$

N-type region:

$n = n_{n0} \approx N_D = 1\times 10^{18}\ cm^{-3}$.

$$p = p_{n0} = n_i^2 / n_{n0} = \left(1.5\times10^{10}\right)^2 / 10^{18} = 2.25\times10^{2}\ cm^{-3}$$

We can calculate the position of the Fermi energy in the quasi-neutral n-type and p-type regions, respectively, using Eq. (3.18a). Let's assume that the reference energy level is the bottom of the conduction band, E_c=0 eV.

N-type region:

$$E_F - E_C = -kT\ln\left(N_C/n\right) = -0.0258\ \ln\left(3.32\times10^{19}/1\times10^{18}\right) = -0.09\,eV$$

P-type region:

$$E_F - E_C = -kT\ln\left(N_C/n\right) = -0.0258\ln\left(3.32\times10^{19}/2.25\times10^{4}\right) = -0.90\,eV$$

The minus sign tells us that the Fermi energy is positioned below the E_c.

The built-in voltage across the p-n junction is calculated using Eq. (4.16)

$$\psi_0 = \frac{kT}{q}\ln\left(\frac{N_A N_D}{n_i^2}\right) = 0.0258\ln\left(10^{16}\times10^{18}/\left(1.5\times10^{10}\right)^2\right) = 0.81V$$

The width of the depletion region is calculated from Eq. (4.18)

$$W = \sqrt{\frac{2\varepsilon_r\varepsilon_0}{q}\psi_0\left(\frac{1}{N_A}+\frac{1}{N_D}\right)} = \sqrt{\frac{2\times11.7\times8.854\times10^{-14}}{1.602\times10^{-19}}\times0.81\times\left(\frac{1}{10^{16}}+\frac{1}{10^{18}}\right)} = 3.25\times10^{-5}\ cm = 0.325\ \mu m$$

A typical thickness of c-Si wafer is 300 µm. The depletion region is 0.3 µm which represents 0.1% of the thickness of the wafer. It is important to realize that almost the whole bulk of the wafer is a quasi-neutral region without the internal electrical field.

The maximum electric field is at the metallurgical junction and is calculated from Eq. (4.19).

$$\xi_{max} = \sqrt{\frac{2q}{\varepsilon_r\varepsilon_0}\psi_0\left(\frac{N_A N_D}{N_A+N_D}\right)} = \sqrt{\frac{2\times1.602\times10^{-19}}{11.7\times8.854\times10^{-14}}\times0.81\times\left(\frac{10^{16}\times10^{18}}{10^{16}+10^{18}}\right)} = 50\times10^{3}\ V\ cm^{-1}$$

4.2.3 *p-n* junction under applied voltage

When an external voltage, V_a, is applied to a *p-n* junction the potential difference between the *n*-type and *p*-type regions will change and the electrostatic potential across the space-charge region will become (ψ_0 - V_a). Remember that under equilibrium the built-in potential is negative in the *p*-type region with respect to the *n*-type region. When the applied external voltage is negative with respect to the potential of the *p*-type region, the applied voltage will increase the potential difference across the *p-n* junction. We refer to this situation as *p-n* junction under reverse-bias voltage. The potential barrier across the junction is increased under reverse-bias voltage, which results in a wider space-charge region. The band diagram of the *p-n* junction under reverse-biased voltage is presented in Figure 4.7a. Under external voltage the *p-n* junction is not under equilibrium any more and the concentrations of electrons and holes are described by the quasi-Fermi energy for electrons, E_{FC}, and the quasi-Fermi energy holes, E_{FV}, respectively. When the applied external voltage is positive with respect to the potential of the *p*-type region, the applied voltage will decrease the potential difference across the *p-n* junction. We refer to this situation as *p-n* junction under forward-bias voltage. The band diagram of the *p-n* junction under forward-biased voltage is presented in Figure 4.7b. The potential barrier across the junction is decreased under forward-bias voltage and the space charge region becomes narrower. The balance between the forces responsible for diffusion (concentration gradient) and drift (electric field) is disturbed. The lowering of the electrostatic potential barrier leads to a higher concentration of minority carriers at the edges of the space-charge region compared to the situation in equilibrium. This process is referred to as minority-carrier ***injection***. This gradient in concentration causes the diffusion of the minority carriers from the edge into the bulk of the quasi-neutral region.

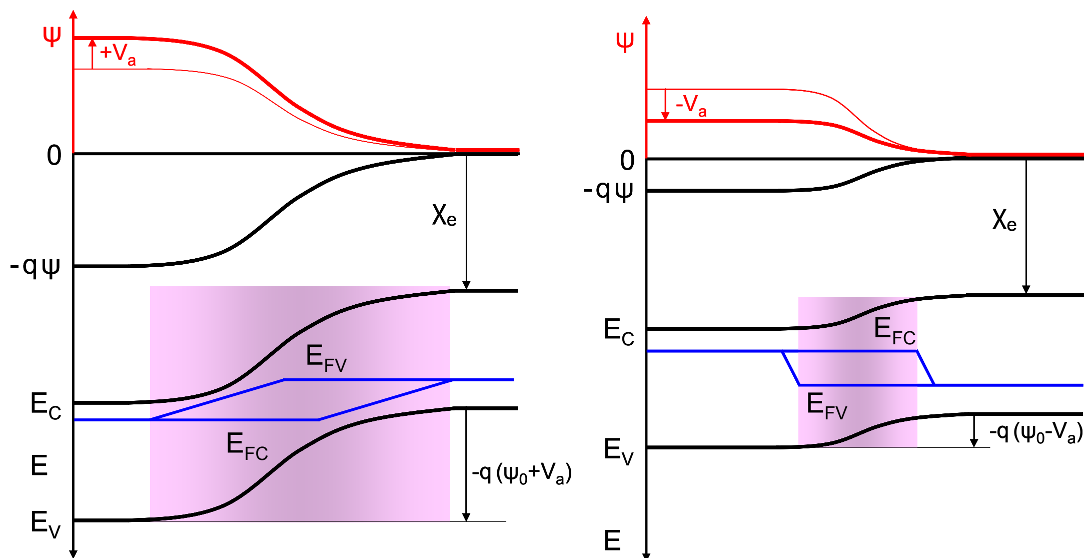

Figure 4.7: Energy band diagram and potential profile (in red colour) of a *p-n* junction under a) reverse bias, and b) forward bias.

The diffusion of minority carriers into the quasi-neutral region causes a so-called ***recombination current***, J_{rec}, since the diffusing minority carriers recombine with the majority carriers in the bulk. The recombination current is compensated by the so-called ***thermal generation current***, J_{gen}, which is caused by the drift of minority carriers, which are present in the corresponding doped regions (electrons in the *p*-type region and holes in the *n*-type region), across the junction. Both, the recombination and generation currents have contributions from electrons and holes. When no voltage is applied to the *p-n* junction, the situation inside the junction can be viewed as the balance between the recombination and generation currents.

$$J = J_{rec} - J_{gen} = 0 \qquad \text{for } V_a = 0 \text{ V} \tag{4.20}$$

It is assumed that when a moderate forward-bias voltage is applied to the junction the recombination current increases with the Boltzmann factor ($\exp(qV_a/kT)$) (*the Boltzmann approximation*):

$$J_{rec}(V_a) = J_{rec}(V_a = 0)\exp\left(\frac{qV_a}{kT}\right) \tag{4.21}$$

On the other hand, the generation current is almost independent of the potential barrier across the junction and is determined by the availability of the thermally-generated minority carriers in the doped regions.

$$J_{gen}(V_a) \approx J_{gen}(V_a = 0) \tag{4.22}$$

The external net-current density can be expressed as

$$J(V_a) = J_{rec}(V_a) - J_{gen}(V_a) = J_0\left[\exp\left(\frac{qV_a}{kT}\right) - 1\right], \tag{4.23}$$

where J_0 is the saturation-current density of the *p-n* junction, given by

$$J_0 = J_{gen}(V_a = 0) \tag{4.24}$$

Eq. (4.23) is known as the ***Shockley equation*** that describes the current-voltage behavior of an ideal *p-n* diode. It is a fundamental equation for microelectronics device physics. The detailed derivation of the dark-current density of the *p-n* junction is carried out in the Appendix 4.4.1 of Chapter 4. The saturation-current density is expressed by Eq. (4.25)

$$J_0 = q\, n_i^2 \left(\frac{D_N}{L_N\, N_A} + \frac{D_P}{L_P\, N_D}\right). \tag{4.25}$$

The saturation-current density depends in a complex way on the fundamental semiconductor parameters. Ideally the saturation-current density should be as low as possible and this requires an optimal and balanced design of the *p*-type and *n*-type semiconductor properties. For example, an increase in the doping concentration decreases the diffusion length of the

minority carriers, which means that the optimal product of these two quantities requires a delicate balance between these two properties.

The recombination of the majority carriers due to the diffusion of the injected minority carriers into the bulk of the quasi-neutral regions results in a lowering of the concentration of the majority carriers compared to the one under equilibrium. The drop in the concentration of the majority carriers is balanced by the flow of the majority carriers from the electrodes into the bulk. In this way the net current flows through the *p-n* junction under forward-bias voltage. For high reverse-bias voltage, the Boltzmann factor in Eq. (4.23) becomes very small and can be neglected. The net current density is given by

$$J(V_a) = -J_0, \qquad (4.26)$$

and represents the flux of thermally generated minority carriers across the junction. The current density-voltage (*J-V*) characteristic of an ideal *p-n* junction is schematically shown in Figure 4.8.

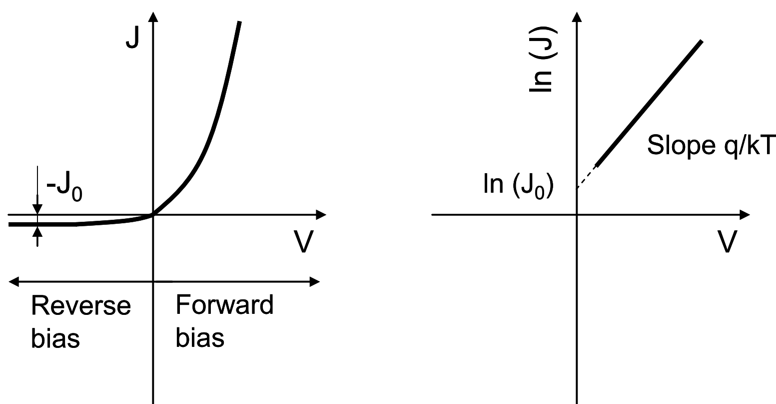

Figure 4.8. *J-V* characteristic of a *p-n* junction; a) linear plot and b) semi-logarithmic plot.

4.2.4 *p-n* junction under illumination

When a *p-n* junction is illuminated the additional electron-hole pairs are generated in the semiconductor. The concentration of minority carriers (electrons in the *p*-type region and holes in the *n*-type region) strongly increases. This increase in the concentration of minority carriers leads to the flow of the minority carriers across the depletion region into the qausi-neutral regions. Electrons flow from the *p*-type into the *n*-type region and holes from the *n*-type into the *p*-type region. The flow of the photo-generated carriers causes the so-called ***photo-generation current***, J_{ph}, which adds to the thermal-generation current, J_{gen}. When no external contact between the *n*-type and the *p*-type regions is established, which means that the junction is in the open-circuit condition, no net current can flow inside the *p-n* junction. It means that the current resulting from the flux of photo-generated and thermally-generated carriers has to be balanced by the opposite recombination current. The recombination current will increase through lowering of the electrostatic potential barrier across the depletion

region. This situation of the illuminated *p-n* junction under open-circuit condition using the band diagram is presented in Figure 4.9a. The electrostatic-potential barrier across the junction is lowered by an amount of V_{oc}. We refer to V_{oc} as the open-circuit voltage. Under non-equilibrium conditions the concentrations of electrons and holes are described by the quasi-Fermi energy levels. It is illustrated in Figure 4.9a that the electrochemical potential of electrons, denoted by E_{FC}, is higher in the n-type region than in the *p*-type region by an amount of $q\ V_{oc}$. This means that a voltmeter will measure a voltage difference of V_{oc} between the contacts of the *p-n* junction. Under illumination, when the *n*-type and *p*-type regions are short circuited, the photo-generated current will also flow through the external circuit. This situation is illustrated in Figure 4.9b. Under the short-circuit condition the electrostatic-potential barrier is not changed, but from a strong variation of the quasi-Fermi levels inside the depletion region one can determine that the current is flowing inside the semiconductor.

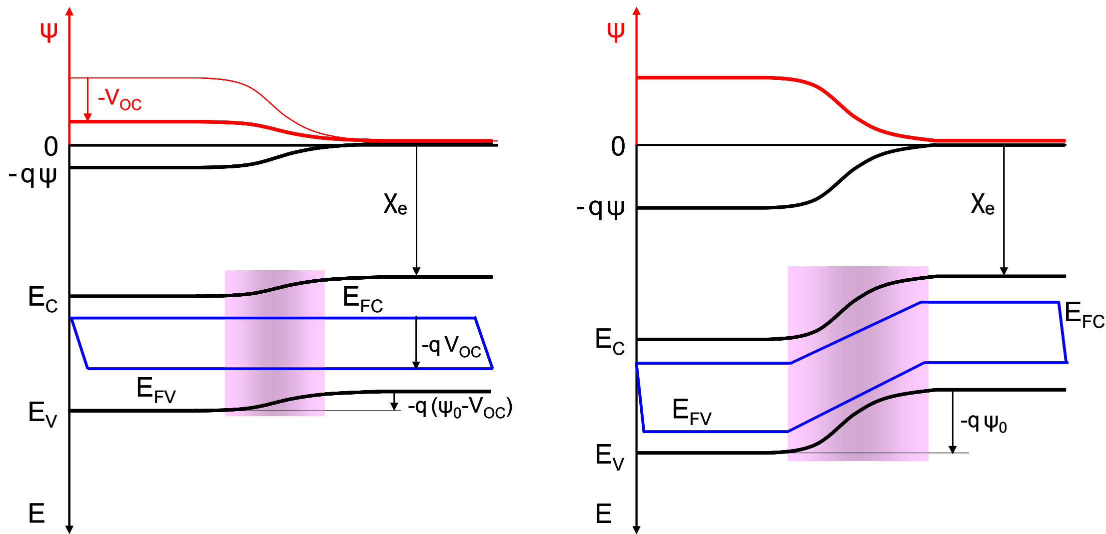

Figure 4.9. Energy band diagram and electrostatic-potential (in red colour) of an illuminated *p-n* junction under the a) open-circuit and b) short-circuit conditions.

When a load is connected between the electrodes of the illuminated *p-n* junction, only a fraction of the photo-generated current will flow through the external circuit. The electro-chemical potential difference between the *n*-type and *p*-type regions will be lowered by a voltage drop over the load. This in turn lowers the electrostatic potential over the depletion region which results in an increase of the recombination current. The net current flowing through the load is determined as the sum of the photo- and thermal generation currents and the recombination current (*the superposition approximation*). The voltage drop at the load can be simulated by applying a forward-bias voltage to the junction, therefore Eqs. (4.23), which describes the behaviour of the junction under applied voltage, is included to describe the net current of the illuminated *p-n* junction:

$$J(V_a) = J_{rec}(V_a) - J_{gen}(V_a) - J_{ph} = J_0\left[\exp\left(\frac{qV_a}{kT}\right) - 1\right] - J_{ph} \tag{4.27}$$

The dark and illuminated *J-V* characteristics of the *p-n* junction are represented in Figure 4.10. Note, that the superposition principle is reflected in Figure 4.10. The illuminated *J-V* characteristic of the *p-n* junction is the same as the dark *J-V* characteristic, but it is shifted down by the photo-generated current density J_{ph}. The detailed derivation of the photo-generated current density of the *p-n* junction is carried out in the Appendix 4.4.2 of Chapter 4 and its value under uniform generation rate, *G*, is

$$J_{ph} = q\,G\left(L_N + W + L_P\right), \tag{4.28}$$

where L_N and L_P is the minority-carrier-diffusion length for electrons and holes, respectively, and *W* is the width of the depletion region. It means only carriers generated in the depletion region and in the regions up to the minority-carrier-diffusion length from the depletion region contribute to the photo-generated current. Eq. (4.28) is useful when designing the thickness of a solar cell. The thickness of the absorber should not be thicker than the region from which the carriers contribute to the photo-generated current.

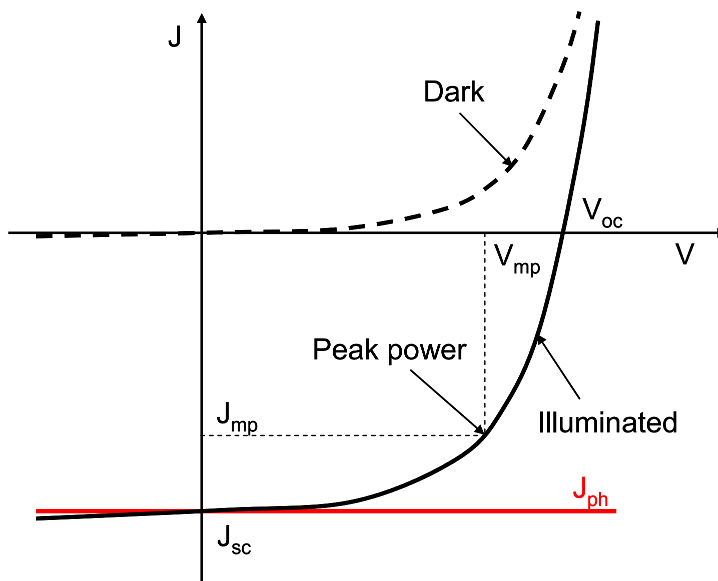

Figure 4.10. *J-V* characteristics of a *p-n* junction in the dark and under illumination.

4.3 Solar cell external parameters

The main parameters that are used to characterize the performance of solar cells are the short-circuit current density, J_{sc}, the open-circuit voltage, V_{oc} and the fill factor, *FF*. These parameters are determined from the illuminated *J-V* characteristic as illustrated in Figure 4.10. The conversion efficiency, η, is determined from these parameters. The short-circuit current is the current that flows through the external circuit when the electrodes of the solar cell are short circuited. In the ideal case, J_{sc} is equal to the photo-generated current density J_{ph}. The open-circuit voltage is the voltage at which no current flows through the external circuit. In this case the dark current compensates the photo-current. The open-circuit voltage

depends on the photo-generated current density and can be calculated from Eq. (4.26) assuming that the net current is zero.

$$V_{oc} = \frac{kT}{q} \ln\left(\frac{J_{ph}}{J_0} + 1 \right) \tag{4.29}$$

The fill factor is the ratio between the maximum power ($P_m = J_{mp} \times V_{mp}$) deliverable by a solar cell and the product of V_{oc} and J_{sc}.

$$FF = \frac{J_{mp} V_{mp}}{J_{sc} V_{oc}} \tag{4.30}$$

In case that the solar cell behaves as an ideal diode the fill factor can be expressed as a function of open-circuit voltage[3].

$$FF = \frac{v_{oc} - \ln(v_{oc} + 0.72)}{v_{oc} + 1}, \tag{4.31}$$

where $v_{oc} = V_{oc} / (kT/q)$ is a normalized voltage.

The conversion efficiency is calculated as the ratio between the generated maximum power and the incident power. The irradiance value, P_{in}, of 1000 W/m^2 of AM1.5 spectrum has become a standard for measuring the conversion efficiency of solar cells.

$$\eta = \frac{P_m}{P_{in}} = \frac{J_{mp} V_{mp}}{P_{in}} = \frac{J_{sc} V_{oc} FF}{P_{in}} \tag{4.32}$$

Typical external parameters of a crystalline silicon solar cell as shown in Figure 3.1 are; J_{sc} of 35 mA/cm^2, V_{oc} up to 0.65 V and FF in the range 0.75 to 0.80. The conversion efficiency lies in the range of 17 to 18%.

[3] M.A. Green, Solar Cells; Operating Principles, Technology and System Applications, Prentice-Hall, 1982.

EXAMPLE

A crystalline silicon solar cell generates a photo-current density J_{ph} = 35 mA/cm^2. The wafer is doped with 1×10^{17} acceptor atoms per cubic centimeter and the emitter layer is formed with a uniform concentration of 1×10^{19} donors per cubic centimeter. The minority-carrier diffusion length in the p-type region and n-type region is 500×10^{-6} m and 10×10^{-6} m, respectively.

The intrinsic carrier concentration in silicon at 300 K is 1.5×10^{10} cm^{-3}, the mobility of electrons in the p-type region is μ_n = 1000 cm^{2}V^{-1}s^{-1} and holes in the n-type region is μ_p = 100 cm^{2}V^{-1}s^{-1}.

Assume that the solar cell behaves as an ideal diode. Calculate the open-circuit voltage and the conversion efficiency of the cell.

$J_{ph} = 350\ A/m^2$.
$N_A = 1\times10^{17}\ cm^{-3} = 1\times10^{23}\ m^{-3}$.
$N_D = 1\times10^{19}\ cm^{-3} = 1\times10^{25}\ m^{-3}$.
$L_N = 500\times10^{-6}\ m$.
$L_P = 10\times 10^{-6}\ m$.
$D_N = (kT/q)\ \mu_n = 0.0258\ V \times 1000\times10^{-4}\ m^2V^{-1}s^{-1} = 2.58\times10^{-3}\ m^2s^{-1}$.
$D_P = (kT/q)\ \mu_p = 0.0258\ V \times 100\times10^{-4}\ m^2V^{-1}s^{-1} = 0.258\times10^{-3}\ m^2s^{-1}$.

According to the assumption the solar cell behaves as an ideal diode, it means that the Shockley equation describing the J-V characteristic is applicable. Using Eq. (4.25) we determine the saturation-current density:

$$J_0 = qn_i^2\left(\frac{D_N}{L_N N_A} + \frac{D_P}{L_P N_D}\right)$$

$J_0 = (1.602\times10^{-19}\ C \times (1.5\times10^{16})^2\ m^{-6}) \times$
$[(2.58\times10^{-3}\ m^2s^{-1}/(500\times10^{-6}\ m \times 1\times10^{23}\ m^{-3})) + (0.258\times10^{-3}\ m^2s^{-1}/(10\times10^{-6}\ m \times 1\times10^{25}\ m^{-3}))] =$
$3.6\times10^{13}\ C\ m^{-6} \times [(5.16\times10^{-23} + 2.58\times10^{-24})\ m^4s^{-1}] = 1.95\times10^{-9}\ C\ s^{-1}m^{-2} = 1.95\times10^{-9}\ Am^{-2}$

Using Eq. (4.29) we determine the open-circuit voltage:

$$V_{oc} = \frac{kT}{q}\ln\left(\frac{J_{ph}}{J_0} + 1\right)$$

$V_{oc} = 0.0258\ V \times \ln((350\ Am^{-2}/\ 1.95\times10^{-9}\ Am^{-2}) + 1) = 0.67\ V$

The fill factor of the cell can be calculated from Eq. (4.31). First we normalize the V_{oc}.

$v_{oc} = V_{oc}/(kT/q) = 0.67\ V/0.0258\ V = 26.8$

$$FF = \frac{v_{oc} - \ln(v_{oc} + 0.72)}{v_{oc} + 1}$$

$FF = (26.8 - \ln(26.8+0.72))/(26.8+1) = 0.84$

The conversion efficiency is determined using Eq. (4.32)

$$\eta = \frac{J_{sc} V_{oc} FF}{P_{in}}$$

$\eta = (350\ Am^{-2} \times 0.67\ V \times 0.84)/1000\ W\ m^{-2} = 0.197$
$\eta = 19.7\%$

4.4 Appendix

4.4.1 Derivation of *J-V* characteristic in dark

When an external voltage, V_a, is applied to a *p-n* junction the potential difference between the *n*-type and *p*-type regions will change and the electrostatic potential across the space-charge region will become (ψ_0 - V_a). Under the forward-bias condition an applied external voltage decreases the electrostatic-potential difference across the *p-n* junction. The concentration of the minority carriers at the edge of the space-charge region increases exponentially with the applied forward-bias voltage but it is still much lower that the concentration of the majority carriers (*low-injection conditions*). The concentration of the majority carriers in the quasi-neutral regions do not change significantly under forward bias. The concentration of charge carriers in a *p-n* junction under forward bias is schematically presented in Figure 4.11.

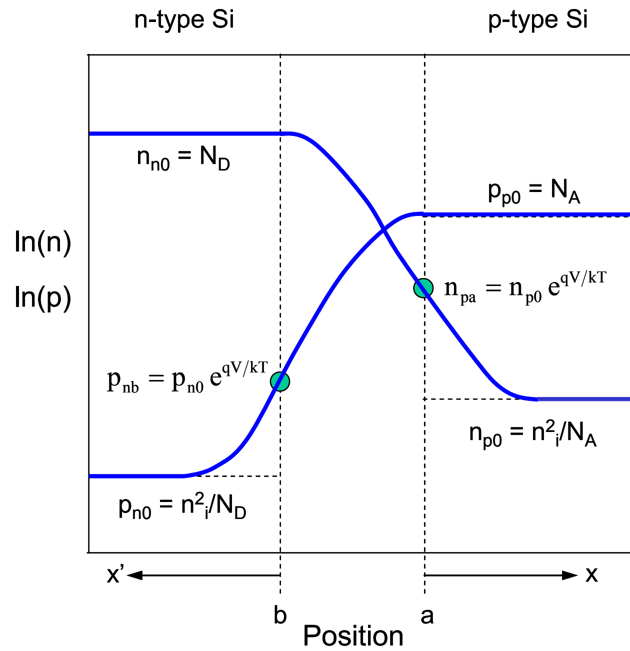

Figure 4.11. Concentration profiles of mobile charge carriers in a *p-n* junction under forward bias (blue line). Concentration profiles of carriers under thermal equilibrium are shown for comparison (black line).

The concentrations of the minority carriers at the edges of the space-charge region, electrons in the *p*-type semiconductor and holes in the *n*-type semiconductor after applying forward-bias voltage are described by Eq. (4.33a) and Eq. (4.33b), respectively.

$$n_{pb} = n_{p0} \exp\left[qV_a/kT\right] = \frac{n_i^2}{N_A} \exp\left[qV_a/kT\right] \tag{4.33a}$$

$$p_{na} = p_{n0} \exp[qV_a/kT] = \frac{n_i^2}{N_D} \exp[qV_a/kT] \quad (4.33b)$$

Since it is assumed that there is no electric field in the quasi-neutral region the current-density equations of carriers reduce to only diffusion terms and are not coupled by the electric field. The current is based on the diffusive flows of carriers in the quasi-neutral regions and is determined by the diffusion of the minority carriers. The minority-carriers concentration can be calculated separately for both quasi-neutral regions. The electron-current density in the quasi-neutral region of the *p*-type semiconductor and the hole-current density in the quasi-neutral region of the *n*-type semiconductor are described by Eq. (4.34a) and Eq. (4.34b), respectively.

$$J_N = qD_N \frac{dn}{dx} \quad (4.34a)$$

$$J_P = -qD_P \frac{dp}{dx} \quad (4.34b)$$

The continuity equations (Eq. 3.54) for electrons and holes in steady-state ($\partial n/\partial t = 0$ and $\partial p/\partial t = 0$) can be written as

$$\frac{1}{q}\frac{dJ_N}{dx} - R_N + G_N = 0 \quad (4.35a)$$

$$-\frac{1}{q}\frac{dJ_P}{dx} - R_P + G_P = 0 \quad (4.35b)$$

Under *low-injection conditions*, a change in the concentration of the majority carriers due to generation and recombination can be neglected. However, the recombination-generation rate of minority carriers depends strongly on the injection and is proportional to the excess of minority carriers at the edges of the depletion region. The recombination-generation rate of electrons, R_N, in the *p*-type semiconductor and holes, R_P, in the *n*-type semiconductor is described by Eq. (3.29a) and Eq. (3.29b), respectively,

$$R_N = \frac{\Delta n}{\tau_n} \quad (4.36a)$$

$$R_P = \frac{\Delta p}{\tau_p}, \quad (4.36b)$$

where Δn is the excess concentration of electrons in the *p*-type semiconductor with respect to the equilibrium concentration n_{p0} and τ_n is the electrons (minority carriers) lifetime and Δp is the excess concentration of holes in the *n*-type semiconductor with respect to the equilibrium concentration p_{n0} and τ_p is the holes (minority carriers) lifetime. Δn and Δp are given by Eq. (4.37a) and Eq. (4.37b), respectively,

$$\Delta n = n_p(x) - n_{p0} \tag{4.37a}$$

$$\Delta p = p_n(x) - p_{n0} \tag{4.37b}$$

Combining Eq. (4.35a) with Eq. (4.34a) and Eq. (4.36a) results in Eq. (4.38a) that describes the diffusion of electrons in the *p*-type semiconductor, while combining Eq. (4.35b) with Eq. (4.34b) and Eq. (4.36b) results in Eq. (4.38b) that describes the diffusion of holes in the *n*-type semiconductor

$$D_N \frac{d^2 n_p(x)}{dx^2} = \frac{\Delta n}{\tau_n} - G_N \tag{4.38a}$$

$$D_P \frac{d^2 p_n(x)}{dx^2} = \frac{\Delta p}{\tau_p} - G_P \tag{4.38b}$$

Substituting $n_p(x)$ from Eq. (4.37a) and $p_n(x)$ from Eq. (4.37b) into Eq. (4.38a) and Eq. (4.38b), respectively, knowing that $d^2 n_{p0} / dx^2 = 0$, $d^2 p_{n0} / dx^2 = 0$ and in dark $G_N = G_P = 0$, Eqs. (4.38a) and Eq. (4.38b) simplify to

$$\frac{d^2 \Delta n}{dx^2} = \frac{\Delta n}{D_N \tau_n} \tag{4.39a}$$

$$\frac{d^2 \Delta p}{dx^2} = \frac{\Delta p}{D_P \tau_p} \tag{4.39b}$$

The electron-concentration profile in the quasi-neutral region of the *p*-type semiconductor is given by the general solution to Eq. (4.39a):

$$\Delta n(x) = A \exp\left(\frac{x}{L_N}\right) + B \exp\left(-\frac{x}{L_N}\right) \tag{4.40a}$$

where $L_N = \sqrt{D_N \tau_n}$ (Eq. (3.30a)) is the electron minority-carrier diffusion length. The starting point of the x axis is defined at the edge of the depletion region in the *p*-type semiconductor and denoted as a (see Figure 4.11). The infinite thickness of the *p*-type semiconductor is assumed (*approximation of the infinite thickness*). The constants *A* and *B* can be determined from the boundary conditions:

1. At $x = 0$, $n_{pa} = n_{p0} \exp(qV_a / kT)$,
2. n_p is finite at $x \to \infty$, therefore $A = 0$.

Using the boundary conditions the solution for the concentration profile of electrons in the *p*-type quasi-neutral region is

$$n_p(x) = n_{p0} + n_{p0}\left[\exp\left(\frac{qV_a}{kT}\right) - 1\right]\exp\left(-\frac{x}{L_N}\right), \tag{4.41a}$$

The hole concentration profile in the quasi-neutral region of the *n*-type semiconductor is given by the general solution to Eq. (4.39b):

$$\Delta p(x') = A'\exp\left(\frac{x'}{L_P}\right) + B'\exp\left(-\frac{x'}{L_P}\right) \tag{4.40b}$$

where $L_P = \sqrt{D_P \tau_p}$ (Eq. (3.30b)) is the hole minority-carrier diffusion length. The starting point of the x' axis ($x' = -x$) is defined at the edge of the depletion region in the *n*-type semiconductor and denoted as b (see Figure 4.11). The infinite thickness of the *n*-type semiconductor is assumed (*approximation of the infinite thickness*). The constants A' and B' can be determined from the boundary conditions:

1. At $x' = 0$, $p_{nb} = p_{n0}\exp(qV_a/kT)$,
2. p_n is finite at $x' \to \infty$, therefore $A' = 0$.

The concentration profile of holes in the quasi-neutral region of the *n*-type semiconductor is described by Eq. (4.41b).

$$p_n(x') = p_{n0} + p_{n0}\left[\exp\left(\frac{qV_a}{kT}\right) - 1\right]\exp\left(-\frac{x'}{L_P}\right) \tag{4.41b}$$

When substituting the corresponding concentration profiles of minority carriers (Eq. (4.41)) into Eq. (4.34) one obtains for the current densities:

$$J_N(x) = \frac{qD_N n_{p0}}{L_N}\left[\exp\left(\frac{qV_a}{kT}\right) - 1\right]\exp\left(-\frac{x}{L_N}\right) \tag{4.42a}$$

$$J_P(x') = \frac{qD_P p_{n0}}{L_P}\left[\exp\left(\frac{qV_a}{kT}\right) - 1\right]\exp\left(-\frac{x'}{L_P}\right) \tag{4.42b}$$

Under assumption that the effect of recombination and thermal generation of carriers in the depletion region can be neglected, which means that the electron and hole current densities are essentially constant across the depletion region, one can write for the current densities at the edges of the depletion region

$$J_N\big|_{x=0} = J_N\big|_{x'=0} = \frac{qD_N n_{p0}}{L_N}\left[\exp\left(\frac{qV_a}{kT}\right) - 1\right] \tag{4.43a}$$

$$J_P\big|_{x'=0} = J_P\big|_{x=0} = \frac{qD_P\,p_{n0}}{L_P}\left[\exp\left(\frac{qV_a}{kT}\right)-1\right] \tag{4.43b}$$

The total current density flowing through the *p-n* junction at the steady state is constant across the device therefore we can determine the total current density as the sum of the electron and hole current densities at the edges of the depletion region:

$$J(V_a) = J_N\big|_{x=0} + J_P\big|_{x=0} = \left(\frac{qD_N n_{p0}}{L_N} + \frac{qD_P\,p_{n0}}{L_P}\right)\left[\exp\left(\frac{qV_a}{kT}\right)-1\right] \tag{4.44}$$

Using Eq. (4.2b) and Eq. (4.1b), Eq. (4.44) can be rewritten as

$$J(V_a) = J_0\left[\exp\left(\frac{qV_a}{kT}\right)-1\right] \tag{4.45}$$

where J_0 is the saturation-current density of the *p-n* junction which is given by Eq. (4.46)

$$J_0 = \left(\frac{qD_N n_i^2}{L_N\,N_A} + \frac{qD_P\,n_i^2}{L_P\,N_D}\right) \tag{4.46}$$

Eq. (4.45) is known as the ***Shockley equation*** that describes the current-voltage behaviour of an ideal *p-n* diode. It is a fundamental equation for microelectronics device physics.

4.4.2 Derivation of *J-V* characteristic under illumination

When a *p-n* junction is illuminated the additional electron-hole pairs are generated through the junction. In case of moderate illumination the concentration of majority carriers does not change significantly while the concentration of minority carriers (electrons in the *p*-type region and holes in the *n*-type region) will strongly increase. In the following section it is assumed that the photo-generation rate, G, is uniform throughout the *p-n* junction (*uniform generation-rate approximation*). This assumption reflects a situation when the device is illuminated with a long-wavelength light which is weakly absorbed by the semiconductor. The concentration of charge carriers in a *p-n* junction with uniform photo-generation rate is schematically presented in Figure 4.12.

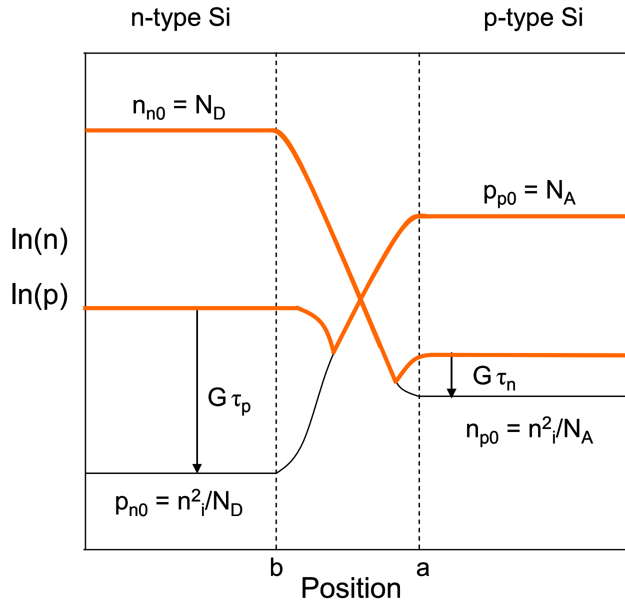

Figure 4.12: Concentration profiles of mobile charge carriers in an illuminated *p-n* junction with uniform generation rate G (orange line). Concentration profiles of charge carriers under equilibrium conditions are shown for comparison (black line).

Eqs. (4.38) describe the steady-state situation for minority carriers when the junction is illuminated. In this case the generation rate is not zero and the equation can be rewritten to

$$\frac{d^2\Delta n}{dx^2} = \frac{\Delta n}{D_N \tau_n} - \frac{G}{D_N} \tag{4.47a}$$

$$\frac{d^2\Delta p}{dx^2} = \frac{\Delta p}{D_P \tau_p} - \frac{G}{D_P} \tag{4.47b}$$

Under the assumption that G/D_N and G/D_P are constant, the general solution to Eq. (4.47) is

$$\Delta n(x) = G\tau_n + C\exp\left(\frac{x}{L_N}\right) + D\exp\left(-\frac{x}{L_N}\right) \quad (4.48a)$$

$$\Delta p(x') = G\tau_p + C'\exp\left(\frac{x'}{L_P}\right) + D'\exp\left(-\frac{x'}{L_P}\right) \quad (4.48b)$$

The constants in the Eqs. (4.48) can be determined from the same boundary conditions as were used in the analysis of the *p-n* junction in dark. The particular solution for the concentration profile of electrons in the quasi-neutral region of the *p*-type semiconductor and holes in the quasi-neutral region of the *n*-type semiconductor is described by Eq. (4.49a) and Eq. (4.49b), respectively.

$$n_p(x) = n_{p0} + G\tau_n + \left[n_{p0}\left(\exp\left(\frac{qV}{kT}\right)-1\right) - G\tau_n\right]\exp\left(-\frac{x}{L_N}\right) \quad (4.49a)$$

$$p_n(x') = p_{n0} + G\tau_p + \left[p_{n0}\left(\exp\left(\frac{qV}{kT}\right)-1\right) - G\tau_p\right]\exp\left(-\frac{x'}{L_P}\right) \quad (4.49b)$$

When substituting the corresponding concentration profiles of minority carriers (Eq. (4.49)) into Eq. (4.34) one obtains for the current densities:

$$J_N(x) = \frac{qD_N n_{p0}}{L_N}\left[\exp\left(\frac{qV}{kT}\right)-1\right]\exp\left(-\frac{x}{L_N}\right) - qGL_N\exp\left(-\frac{x}{L_N}\right) \quad (4.50a)$$

$$J_P(x') = \frac{qD_P p_{n0}}{L_P}\left[\exp\left(\frac{qV}{kT}\right)-1\right]\exp\left(-\frac{x'}{L_P}\right) - qGL_P\exp\left(-\frac{x'}{L_P}\right) \quad (4.50b)$$

In case of ideal *p-n* junction the effect of recombination in the depletion region was neglected. However, the contribution of photo-generated charge carriers to the current in the depletion region has to be taken into account. The contribution of optical generation from the depletion region to the current density is given by

$$J_N\big|_{x=0} = q\int_{-W}^{0}(-G)\,dx = -qGW \quad (4.51a)$$

$$J_P\big|_{x'=0} = q\int_{-W}^{0}(-G)\,dx' = -qGW \quad (4.51b)$$

The total current density flowing through the *p-n* junction in the steady state is constant across the junction therefore we can determine the total current density as the sum of the electron and hole current densities at the edges of the depletion region (the superposition approximation):

$$J(V_a) = J_N\big|_{x=0} + J_P\big|_{x=0} = \left(\frac{qD_N n_{p0}}{L_N} + \frac{qD_P\, p_{n0}}{L_P}\right)\left[\exp\left(\frac{qV_a}{kT}\right) - 1\right] - qG(L_N + L_P + W) \quad (4.52)$$

Eq. (4.52) can be rewritten as

$$J(V_a) = J_0\left[\exp\left(\frac{qV_a}{kT}\right) - 1\right] - J_{ph}, \quad (4.53)$$

where J_{ph} is the photo-current expressed by Eq. 4.28

$$J_{ph} = qG\left(L_N + W + L_P\right)$$

A number of approximations have been made in order to derive the analytical expressions for the current-voltage characteristics of an ideal *p-n* junction in dark and under illumination. The approximations are summarized below:

- The depletion-region approximation
- The Boltzmann approximation
- Low-injection conditions
- The superposition principle
- Infinite thickness of doped regions
- Uniform generation rate

The derived expressions describe the behaviour of an ideal *p-n* junction and help to understand the basic processes behind the operation of the *p-n* junction, but they do not fully and correctly describe practical *p-n* junctions. For example, the thickness of a *p-n* junction is limited, which means that the recombination at the surface of the doped regions has to be taken into account. The thinner a *p-n* junction is, the more important the surface recombination becomes. The surface recombination modifies the value of the saturation-current density. Further it was assumed that there are no recombination-generation processes in the depletion region. However, in real *p-n* junctions, the recombination in the depletion region represents a substantial loss mechanism. These and other losses in a solar cell are discussed in Chapter 5.